9-1-2004

Intersection of a domains in the c-domain matrix driven by electric field in tetragonal ferroelectric crystal

Xiaoli Tan
Iowa State University, xtan@iastate.edu

J. K. Shang
University of Illinois at Urbana-Champaign

Intersection of a domains in the c-domain matrix driven by electric field in tetragonal ferroelectric crystal

Abstract
Domain structures in a tetragonal ferroelectric crystal were examined by transmission electron microscopy(TEM) before and after application of bipolar cyclic electric fields. Prior to the application of the bipolar field, the crystal was poled to an initial domain structure which consisted of a high volume fraction of c domains. Dispersed in the matrix of the c domains were two orthogonal sets of a-domain strips. These two sets of a-domain strips stayed apart to avoid direct contact. Upon application of bipolar cyclic electric fields, intersections of the a domains were observed in the 〈001〉-oriented tetragonal ferroelectric crystal. These intersections were formed as one set of the a domains grew under the influence of the in-plane electric field. As a result of the domain wall intersection, segments of the domain wall between two intersecting a domains carried excess electric charges. In the successive TEM examination, domain wall distortion and microcracks were found at these intersections.

Keywords
Domain walls, Polarization, Ferroelectric domain structure, Crystal structure, Transmission electron microscopy, Piezoelectric fields, Electric fields, Lead, Ozone, Single crystals

Disciplines
Materials Science and Engineering

Comments
The following article appeared in *Journal of Applied Physics* 96 (2004): 2805 and may be found at http://dx.doi.org/10.1063/1.1775307.

Intersection of a domains in the c -domain matrix driven by electric field in tetragonal ferroelectric crystal

X. Tan and J. K. Shang

Citation: Journal of Applied Physics **96**, 2805 (2004); doi: 10.1063/1.1775307
View online: http://dx.doi.org/10.1063/1.1775307
View Table of Contents: http://scitation.aip.org/content/aip/journal/jap/96/5?ver=pdfcov
Published by the AIP Publishing

Intersection of *a* domains in the *c*-domain matrix driven by electric field in tetragonal ferroelectric crystal

X. Tan[a)]
Department of Materials Science and Engineering, Iowa State University, Ames, Iowa 50011

J. K. Shang
Department of Materials Science and Engineering, University of Illinois at Urbana-Champaign, Urbana, Illinois 61801

(Received 5 March 2004; accepted 30 May 2004)

Domain structures in a tetragonal ferroelectric crystal were examined by transmission electron microscopy (TEM) before and after application of bipolar cyclic electric fields. Prior to the application of the bipolar field, the crystal was poled to an initial domain structure which consisted of a high volume fraction of *c* domains. Dispersed in the matrix of the *c* domains were two orthogonal sets of *a*-domain strips. These two sets of *a*-domain strips stayed apart to avoid direct contact. Upon application of bipolar cyclic electric fields, intersections of the *a* domains were observed in the ⟨001⟩-oriented tetragonal ferroelectric crystal. These intersections were formed as one set of the *a* domains grew under the influence of the in-plane electric field. As a result of the domain wall intersection, segments of the domain wall between two intersecting *a* domains carried excess electric charges. In the successive TEM examination, domain wall distortion and microcracks were found at these intersections. © *2004 American Institute of Physics*. [DOI: 10.1063/1.1775307]

I. INTRODUCTION

Ferroelectric domains are the volume units with homogeneous electrical polarization. They respond to external electrical stimulus by the expansion of domains with favored polarization orientations. Domain walls and domain configurations are well known to contribute significantly to dielectric and piezoelectric properties of solids. In barium titanate ceramics, domain wall motion accounted for as much as 40% of the increase in the dielectric constant.[1] In $Pb(Mg_{1/3}Nb_{2/3})O_3$-$PbTiO_3$ (PMN-PT) and $Pb(Zn_{1/3}Nb_{2/3})O_3$-$PbTiO_3$ (PZN-PT) single crystals, ultrahigh piezoelectric properties were observed only in domain engineered crystals with a multidomain state.[2–4] Therefore, understanding of domain wall configuration and movement is important to development of ferroelectric materials with high dielectric and piezoelectric properties and to design of ferroelectric devices.

In the as-grown or poled state, domain structures follow a set of well-established rules in common ferroelectrics.[5] However, movement of domain walls under an external field often results in the dynamic transformation of an initial simple domain structure into a complex domain configuration. The complex domain structures may include intersecting domain walls.[6–10] As a result of the domain intersection, electric as well as mechanical complications may arise in the ferroelectric response of a multidomained structure. To the electric behavior, the domain intersection carries excess electrical charges and thus provides a convenient path for charge injection which in turn may cause electric fatigue.[10] To the mechanical response, the intersection produces local lattice distortion, which may result in changes in domain wall density[7] or local fracture.[11]

The domain intersections have been observed in both single crystals[9–15] and polycrystalline ceramics.[6–8] These intersections clearly violate the established rules for domain structures by allowing charged domain walls. However, it is not clear if a new set of rules, if any, may govern intersections of ferroelectric domains. The lack of structural information in the early reports of domain intersection makes it difficult to analyze the detailed structure of the intersection. Accordingly, the objective of the present study was to conduct a systematic examination of the domain structure involved in the intersections so that ultimately the rules for dynamic transformation of domain structures may be established.

In literature, ferroelectric domains in tetragonal crystals are often grouped as *a* domains and *c* domains, depending on the direction of their polarization vectors with respect to the crystal surface.[8] In the TEM examination of a ⟨001⟩-oriented tetragonal crystal specimen, 90° domain walls separating two *a* domains have different appearance from that separating an *a* domain from a *c* domain. The *a*/*a*-domain wall produces the contrast of a thin line but the inclined *a*/*c* domain wall appears with fringe contrast.[16] Recently, we reported two cases of domain intersections between (i) *c* domains with *a* domains in the *a*-domain matrix[16] and (ii) orthogonal *a* domains in the *a*-domain matrix.[17] In case (i), the intersection resulted in formation of partial dislocations and stacking faults. In case (ii), initial domains were divided into smaller cells following the intersection. In the present work, we report the results related to a third configuration involving intersecting *a* domains in the *c*-domain matrix, in which the intersection resulted in microcracking of the ferroelectric crystal.

II. EXPERIMENTAL PROCEDURE

The ferroelectric material used in this study was a single crystal of 0.65PMN-0.35PT. The crystal was grown with a

[a)]Electronic mail: xtan@iastate.edu

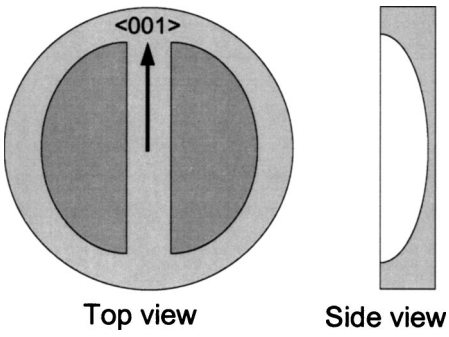

FIG. 1. Illustration of the dimpled {001} foil specimen for bipolar electric-field cycling.

vertical Bridgman method, using a sealed platinum crucible by (110) seeding. A thin {001} slice was cut from the crystal according to the predetermined orientation by x-ray Laue method. The thin slice was subsequently poled along thickness direction. The poled slice was then ground and polished to a final thickness around 120 μm. X-ray Laue camera was used again to confirm the plane normal direction and determine the in-plane orientations. The crystal symmetry and domain polarization were analyzed with an x-ray diffractometer.

Disks of 3 mm diameter were ultrasonically cut from the thin slice and the central areas of the disks were further thinned to about 15 μm by mechanical dimpling. The dimpled specimens were annealed at 250 °C for 1 h to minimize residual stresses. These annealed disks were checked again with the x-ray diffractometer for possible polarization switching during specimen preparation. Two half-circle-shaped Au films were then evaporated onto the flat surface of the specimen with a gap about 500 μm along the $\langle 100 \rangle$ direction, as schematically illustrated in Fig. 1. Cyclic bipolar electric fields with an amplitude of ±6.5 kV/cm were applied to the electroded specimen for 5×10^6 cycles. An optical microscope with cross-polarized light was used to monitor the domain morphology change. The cycled specimen was then ion milled at 5 kV with 12° incidence angle until the occurrence of a central perforation. Detailed analysis of the domain intersections was carried out with a Phillips CM-12 TEM operated at 120 kV.

III. RESULTS

A. Matrix of *c* domains

For observation of intersecting *a* domains in the *c*-domain matrix, the crystal should contain a high volume fraction of *c* domains. This was realized by applying a static electric field to pole the thin {001} crystal along the thickness direction. After poling, the thin slice specimen was analyzed by x-ray diffraction. As shown in Fig. 2, the (002) peak was very strong, indicating that *c* domains occupied most volume of the specimen. This is consistent with optical microscopy examinations, where regular domain strips were not found. The splitting of {002} peak was due to the tetragonal symmetry. Figure 2 also shows the diffraction spectrum for the dimpled and annealed 3-mm disks. A slightly higher (200) peak pointed to an increased amount of *a* domains.

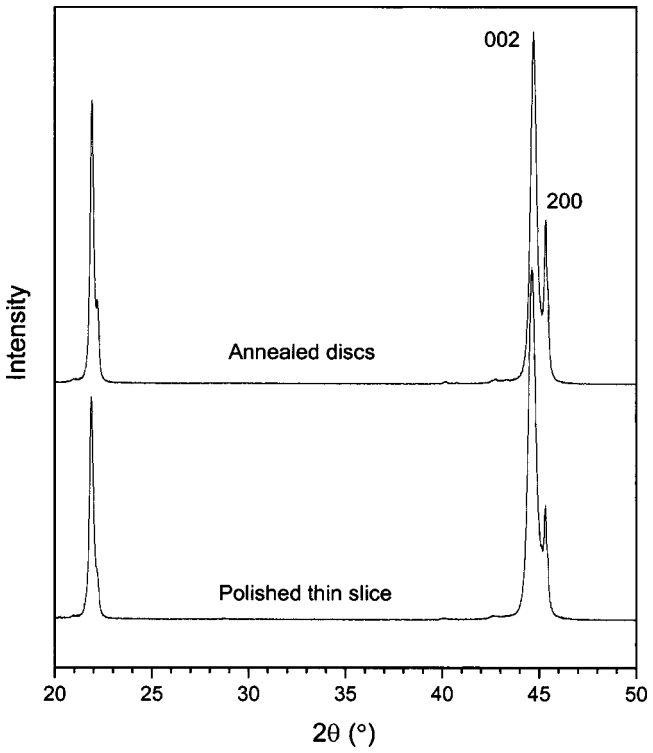

FIG. 2. X-ray diffraction spectrum reveals a high volume fraction of *c* domains with out-of-plane polarization. The peak splitting confirms the tetragonal structure.

Optical microscopy examination confirmed the presence of two sets of long strips of *a* domains in the central portion of the dimple (images are not shown here). However, these two sets of *a* domains stayed apart and no intersections were found. As expected, all domain walls were parallel to $\langle 010 \rangle$ directions, indicating uncharged {101} permissible wall plane.

B. Optical observations

Observations of domain structure were initially made under optical microscope as the bipolar electric fields were applied along the $\langle 100 \rangle$ direction. At a field amplitude of ±6.5 kV/cm, the *a*-domain strips perpendicular to the applied field expanded along both the length and width directions, while the *a*-domain strips parallel to the applied field direction remained unchanged. The domain structure in the crystal after 5×10^6 electric cycles is shown in Fig. 3, where the bright strips are *a* domains and the darker background is the *c*-domain matrix. The expansion of one set of *a*-domain strips (vertical) along their length direction led to the formation of intersections with the other set of *a*-domain strips (horizontal). In addition to the growth of the vertical set of *a* domains, many fine fringes, running parallel to the vertical domain strips, were present in the large *c* domains. The inset presents a magnified view of the rectangular area in the white box and clearly shows these fringes. These fringes are believed to be *a* domains generated during the electrical cycling. Furthermore, microcracks, as marked A and B in Fig. 3, were observed at some intersections.

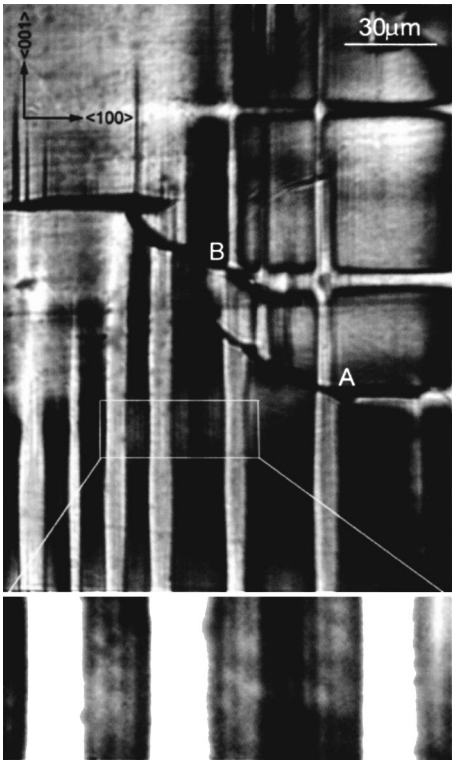

FIG. 3. The morphology of the intersecting *a* domains in the *c*-domain matrix under optical microscopy after extended electrical cycling. The electric-field was applied along the horizontal direction. Vertical fine fringes are evident between wide domains. The bottom part shows the magnified view of the rectangular area in the white box.

C. TEM observations

Since *a* domain and *c* domain are separated by an inclined domain boundary in a ⟨001⟩ oriented thin slice of the crystal, the walls of the *a* domains produced fringe contrast in the TEM when the electron beam is parallel to the [001] direction, as shown in Fig. 4. To verify the out-of-plane polarization vector of the *c*-domain matrix, convergent beam electron diffraction (CBED) pattern was obtained from the *c* domain and is shown in the inset of Fig. 4(b). The fourfold rotational symmetry indicated that the polarization vector was indeed along the thickness of the specimen (or the electron beam). TEM survey of the domain structure of the electrically cycled specimens revealed two groups of domain configurations. In most of the areas examined in the TEM, there was one set of parallel *a*-domain strips. As shown in Fig. 4(a) these domains were about 200 to 300 nm wide, comparable to the width of those fine domains highlighted in the inset of Fig. 3. Among these *a* domains, irregularities in domain walls were common, including domain terminations (marked *A* in the figure), variation in domain width (*B*), distorted domains (*C*), and merge of adjacent domains (*D*).

In other areas, intersecting sets of *a*-domain strips were found. As these domains were forced into direct contact, three separate situations eventually developed, as shown in Figs. 4(b), 5, and 6. When the intersection occurred at the ends of the two intersecting domains, only minor adjustment in the wall configuration was observed for both domains [Fig. 4(b)]. In the second case, shown in Fig. 5, the tip of one domain hit the side of the other domain. The contact caused

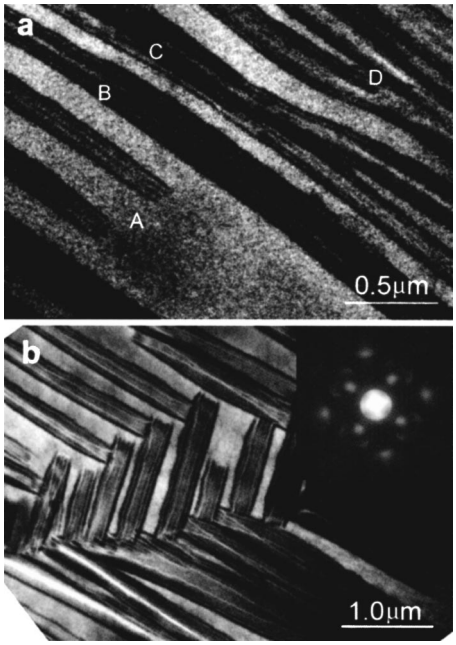

FIG. 4. TEM examination of the electrically cycled specimen: (a) *a* domains in the *c*-domain matrix; (b) the intersecting *a* domains in the *c*-domain matrix. The CBED pattern in the inset verifies the out-of-plane polarization of the matrix domain.

severe deformation of the domain walls as marked by the arrows in Fig. 5(a) and sketched in Fig. 5(b) for clarification. This situation is quite different from the intersection of *c* domain and *a* domain in the *a*-domain matrix [case (i) in the Introduction], where the side of the domain remained undeformed in the TEM observation and partial dislocations appeared at the intersection.[16] The distortion associated with the wall deformation was so severe that domain walls no

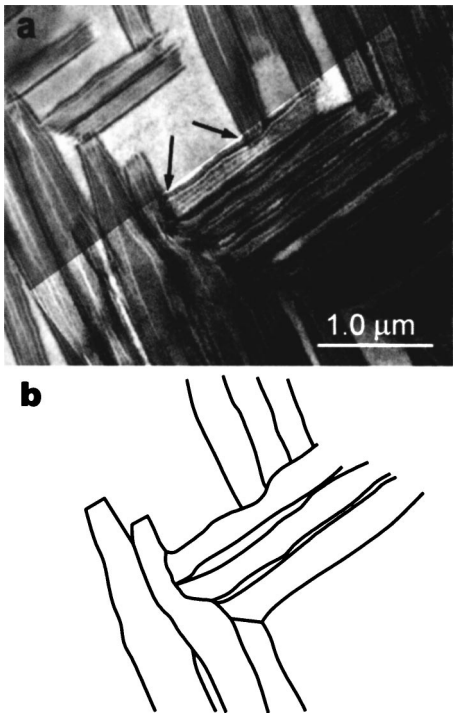

FIG. 5. Domain wall distortion at the intersections: (a) TEM image; (b) sketched domain walls for clarification.

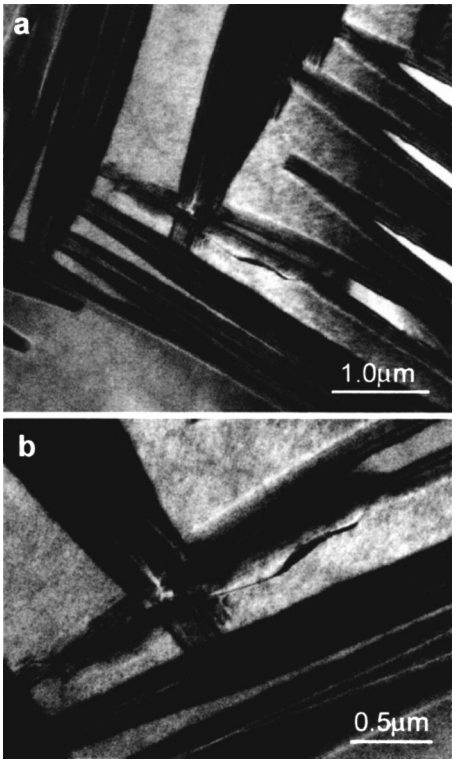

FIG. 6. A microcrack is revealed by TEM at the intersection of two *a* domains in the *c*-domain matrix: (a) domain interpenetration; (b) close examination of the crack.

longer followed the preferred {101} planes. The local angle of intersection varied from acute to obtuse over a wide range.

When one domain attempted to run across the other domain, as shown in Fig. 6, microcrack was produced at the domain intersection. This is so different from the intersection of two *a* domains in the *a*-domain matrix [case (ii) in the Introduction], where interpenetration of the two domains led to the division of a large domain into smaller cells.[17] The center of the crack was roughly at the center of the intersection, suggesting that the crack likely initiated there upon collision of the two domains and extended to about the same distance on both sides of the impact. Further crystallographic analysis found that the crack initially resided on a plane about 15° away from {100} plane but took a deflected path close to the {100} plane subsequently. Such a crack pattern is very different from those produced merely by electric cycling of the crystal, which resulted in crack formation along the domain boundary, i.e., {011} planes in PMN-PT crystals.[18] Since {100} is the preferred cleavage plane for perovskite crystals, and indentation cracks tend to follow {100} planes in PMN-PT crystals,[9] the microcrack at the domain intersection is likely due to internal stresses generated at the domain intersection.

IV. DISCUSSION

A. Formation of intersection

The optical observations showed that the domains responded to the applied bipolar electric field by wall movement and nucleating thin domains. The wall movement resulted in domain switching, which may lead to the

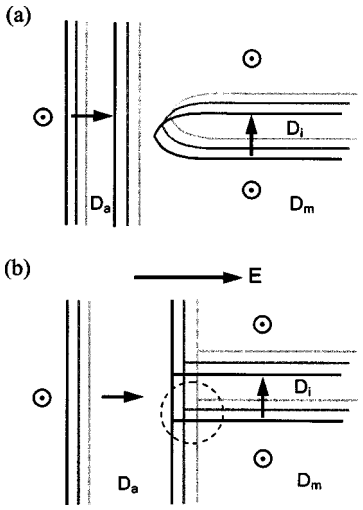

FIG. 7. Diagrams to illustrate the formation of domain intersections shown in Fig. 3: (a) initial configuration; (b) growth of D_a leads to the formation of the intersection.

intersection of two different sets of domains. One mechanism for the formation of the intersection is illustrated in Fig. 7. Initially, the two *a* domains, denoted as D_i and D_a, were not in contact [Fig. 7(a)]. The polarization vectors of these domains were perpendicular to each other, as marked by the two arrows. The matrix *c* domain is denoted as D_m, with polarization vector going out of the plane. To be consistent with the domain configuration in Fig. 3, a polarization vector along the horizontal direction is assigned to D_a while a vector along the vertical direction is assigned to D_i. Such assignment is not only in agreement with crystallographic considerations but also can explain the observed growth of D_a domains under the applied field.

If the electric field is applied along the horizontal direction, as indicated by the long arrow in Fig. 7(b), the D_a domain is favorably oriented because its polarization vector is parallel to the field. In one half cycle (the positive half for convenience), the polarization is in the same direction as the field direction but turns opposite to the field direction in the other half cycle (negative). Therefore, the D_a domain is expected to expand during the positive half cycle. In the following negative half cycle, D_a may respond to the electric field by the 180° domain switching. However, such 180° domain switching is more difficult because of the following arguments. Suppose D_a reversed its polarization to produce a 180° domain switching. If the existing domain wall remained the same, the entire wall would carry excess electric charges, which would raise the electrostatic energy. On the other hand, if the domain wall between D_a and D_m stayed electrically neutral, it would have to rotate by 90°. The domain process then would require both 180° and 90° domain switching.

For D_m and D_i domains, their polarization vectors are 90° away from the field direction. As individuals, D_i or D_m may attempt to align their polarization vectors with the field direction by 90° domain switching. However, when they are grouped side by side as in Fig. 7, 90° domain switching of either one will cause the entire wall between D_i and D_m to be electrically charged. With the given field direction, polariza-

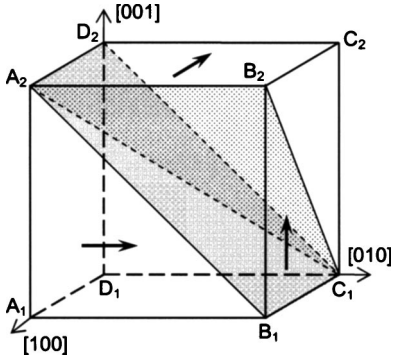

FIG. 8. Schematic illustration of the circled volume in Fig. 7(b). The prism $A_1B_1A_2$-$D_1C_1D_2$ and the pyramid C_1-$A_2B_2C_2D_2$ are the two intersecting *a* domains. The tetrahedron $B_1C_1B_2A_2$ is the matrix *c* domain. The triangle $A_2C_1D_2$ is the electrically charged domain wall segment at the intersection.

tion switching from D_i to D_m or from D_m to D_i is unlikely to occur. Therefore, the morphology of the D_i remained unchanged during electrical cycling, as observed under the optical microscope. On the side of the D_i domain, the D_m domain should also maintain its original polarization. By contrast, part of the D_m domain immediately next to the D_a domain (on the right side) can switch its polarization without incurring any excess electric charge on the domain wall between D_a and D_m domains as long as D_a stays clear of D_i domain or before the intersection occurs. After switching its polarization, this part of the D_m domain will either become part of the D_a domain or form fine *a*-domain strips in the *c*-domain matrix. The former leads to an expansion of the D_a domain as observed in the optical microscope and the latter explains the appearance of fine fringes in Fig. 3. The further expansion of domain D_a during bipolar field cycling then leads to the intersection with the D_i domain, as schematically shown in Fig. 7(b). The mechanism above thus explains the formation of the domain intersection observed in Fig. 3.

B. Electrostatic consideration

When the D_a domain intersects with the D_i domain, part of the domain wall becomes electrically charged. Because of the inclined nature of the two intersecting walls, the structure of the intersection is complex. To illustrate this, Fig. 8 provides a three-dimensional representation of the intersecting domain walls in the circled volume of Fig. 7(b). The prism $A_1B_1A_2$-$D_1C_1D_2$ stands for the D_a domain while the pyramid C_1-$A_2B_2C_2D_2$ represents the D_i. The matrix domain D_m occupies the tetrahedron $B_1C_1B_2A_2$. The neutral position of the domain wall between the two intersecting *a* domains would be plane $D_1B_1B_2D_2$. However, this plane does not share the zone axis C_1A_2 (the intersection line) with other two permissible uncharged walls (triangles $C_1B_2A_2$ and $B_1C_1A_2$). Instead, the domain wall between D_a and D_i assumes the triangular plane $A_2C_1D_2$. This domain wall segment carries electrical charges with a density of $(\sqrt{2}/2)P$, where P is the polarization of the crystal.

In a previous analysis of the domain structure in barium titanate, Krishnan *et al.*[10] suggested that the electrical charges could be avoided by adding a step on the domain wall when two orthogonal *a* domains in the *a*-domain matrix approached each other. However, because the intersection line is not on the electrically neutral plane $D_1B_1B_2D_2$, creating steps on the electrically neutral planes between D_a and D_m domains will not remove charged wall segment from the intersection. The generation of charged wall segments was also found in the other two cases of domain intersection between *a* and *a* domains and between *a* and *c* domains.[16,17] It is therefore a common feature of forced domain intersections. The excess charges on those domain segments along the intersection should directly influence the mobility of the domain walls involved in the intersection.

C. Elastic distortion and microcracking

In tetragonal crystals, 90° domain switching is accompanied by a lattice distortion. The magnitude of the distortion depends on the tetragonality of the crystal structure. For PMN-PT crystal, the c/a ratio was measured to be 1.0135 by x-ray diffraction and the lattice rotation angle θ across a 90° domain wall is thus 0.0134 rad. This corresponds to a lattice distortion strain of 1.3%. When 90° domain walls terminate at a free surface, the distortion is relieved, creating surface lift or offset. However, when these 90° domain walls end at the impinging domain wall in the interior of a crystal, the deformation of the lattice is constrained by the surrounding domains so that high local stresses develop at the intersection. The stresses can cause either deformation of the domain wall locally as shown in Fig. 5 or fracture of the crystal as observed in Fig. 6.

The effect of the local stress may be further understood from the analogy between 90° domain switching and mechanical twinning process since the atomic shifts during a 90° polarization switching in tetragonal crystals are analogous to those produced by the mechanical twinning process. In the case of mechanical twins, the intersection caused distortion of the twin boundary[19] as well as microcracking.[20] Reid[20] analyzed the twin intersections in bcc metals and found that microcracking tended to follow {100} cleavage plane containing the intersecting line. For the *a*- and *a*-domain intersection, the microcrack was also observed very close to the {100} plane, the cleavage plane of perovskite crystals. The slight deviation in the initial crack path from {100} plane may be due to the additional electrostatic energy generated at the ferroelectric domain intersection.

V. CONCLUSIONS

Domain behavior under bipolar electric fields was studied in a ⟨001⟩-oriented tetragonal ferroelectric single crystal. Two sets of nonparallel *a* domains were found to intersect in the *c*-domain matrix after extended electric cycling. The intersection lines were along ⟨111⟩ directions. The intersection created charged domain wall segments between the two *a* domains. When the tip of one domain impacted the side of the other domain, the side of the second domain was severely deformed, resulting in highly distorted domain walls. In the extreme case, one *a* domain was observed to penetrate the other *a* domain. The domain penetration produced microcracking roughly along the {100} cleavage plane of the crys-

tal. When the intersection occurred near the ends of both domains, only minor perturbation to the wall configuration was noted.

ACKNOWLEDGMENTS

The authors would like to acknowledge the financial support by the National Science Foundation through Grant No. CMS-9872306. The experimental work was carried out at the Center for Microanalysis of Materials, University of Illinois, which is supported by the U.S. Department of Energy under Grant No. DEFG02-96-ER45439.

[1]G. Arlt and H. Peusens, Ferroelectrics **48**, 213 (1983).
[2]S. Park and T. R. Shrout, J. Appl. Phys. **82**, 1804 (1997).
[3]S. Wada, S. Park, L. E. Cross, and T. R. Shrout, J. Korean Phys. Soc. **32**, 1290 (1998).
[4]D. Viehland, A. Amin, and J. F. Li, Appl. Phys. Lett. **79**, 1006 (2001).
[5]M. E. Lines and A. M. Glass, *Principles and Applications of Ferroelectrics and Related Materials* (Clarendon Press, Oxford, 1977).
[6]Y. F. Tsun and C. C. Chou, Jpn. J. Appl. Phys., Part 1 **38**, 3585 (1999).
[7]G. Arlt and P. Sasko, J. Appl. Phys. **51**, 4956 (1980).
[8]Y. H. Hu, H. M. Chan, X. W. Zhang, and M. P. Harmer, J. Am. Ceram. Soc. **69**, 594 (1986).
[9]J. K. Shang and X. Tan, Acta Mater. **49**, 2993 (2001).
[10]A. Krishnan, M. E. Bisher, and M. M. J. Treacy, Mater. Res. Soc. Symp. Proc. **541**, 475 (1999).
[11]C. T. A. Suchicital, D. A. Payne, and A. G. de l'Eprevier, in *Proceedings of ISAF'86*, edited by W. A. Smith (IEEE, New York, 1986), p. 465.
[12]B. M. Park and S. J. Chung, J. Am. Ceram. Soc. **77**, 3193 (1994).
[13]C. Chou, C. Chen, and D. Tseng, Mater. Chem. Phys. **45**, 103 (1996).
[14]J. Yin and W. Cao, J. Appl. Phys. **87**, 7438 (2000).
[15]J. Yin and W. Cao, J. Appl. Phys. **92**, 444 (2002).
[16]X. Tan and J. K. Shang, J. Phys.: Condens. Matter **16**, 1455 (2004).
[17]X. Tan and J. K. Shang, J. Appl. Phys. **95**, 635 (2004).
[18]X. Tan, Z. Xu, J. K. Shang, and P. Han, Appl. Phys. Lett. **77**, 1529 (2000).
[19]D. Hull, in *Fracture of Solids*, edited by D. C. Drucker and J. J. Gilman, (Gordon and Breach, New York, 1963), p. 417.
[20]C. N. Reid, Metall. Trans. A **12A**, 371 (1981).